Developmental Biology 448 (2019) 247–259

Contents lists available at ScienceDirect

Developmental Biology

journal homepage: www.elsevier.com/locate/developmentalbiology

Spermatogenesis as a tool for staging gonad development in the gonochoric appendicularian *Oikopleura dioica* Fol 1872

Francesca Cima

Laboratory of Ascidian Biology, Department of Biology, University of Padova, Via Ugo Bassi 58/B, 35121 Padova, Italy

ARTICLE INFO

Keywords:
Appendicularia
Gametogenesis
Male gonad
Oikopleura dioica
Spermatogenesis
Ultrastructure

ABSTRACT

Oikopleura dioica, the only gonochoric species among appendicularians, has a spematozoon with a mid-piece and a conspicuous acrosome that, during fertilisation, undergoes a reaction forming an acrosomal process. To provide more insight into the spermatogenesis of a holoplanktonic tunicate species that completes its life cycle in three to five days, changes in the testis during individual growth have been examined. Spermatogenesis has been subdivided into seven stages based on ultrastructural features during the formation and organisation of the male gonad and the relationships between its macroscopic anatomy and the events of sperm differentiation. Gametes undergo highly synchronised differentiation due to the presence of widespread syncytial structures. Both meiosis and spermiogenesis are brief, and the passage from spermatocytes to spermatids involves a progressive segregation of the germ cells from the syncytial mass with the formation of large cytoplasmic bridges and volume reduction for nucleus compacting and cytoplasmic material changing. The nucleus is small and penetrated anteriorly by a complex acrosome and posteriorly by the distal centriole and part of the flagellum. In spermatids, the single, large mitochondrion appears laterally to the nucleus, and finally, in spermatozoa, it migrates into the mid-piece, wrapping the proximal portion of the axoneme. Because this mitochondrial position is reached only in the late phases of spermatogenesis, it suggests that appendicularians have derived oligopyrenic sperms in which the small nucleus results from adaptation to the assembly of numerous spermatozoa inside the narrow space of the testis compacted in the genital cavity. The formulation of a staging system of gonad development in a model tunicate species known for having the most compacted genome in chordates led to a comparison of histological observations with recent molecular data, improving the characterisation of its biology and life cycle in light of evolutionary implications.

1. Introduction

Appendicularians are planktonic tunicates with low taxonomic diversity and high biomass, the latter of which is produced in a very short time depending on the ranges of nutrient availability and primary production in marine ecosystems closely related to wide fluctuations in both physical factors and environmental resources. This class therefore represents a taxon with 'r-selection', according to the definition of Bretsky and Lorenz (1970), in which high mortality is balanced by high production. These organisms assign the most available resources to their reproduction, maintaining broad areal diffusion and high adaptive ability. *Oikopleura dioica* Fol 1872 is very diffuse in all seas except the Antarctic Ocean and tolerates wide ranges of both temperature and salinity. It is the only appendicularian species found in the Black Sea (Nikitin, 1929), and in the Mediterranean Sea, it is present all year, with two periods of peak abundance, i.e., early spring and summer. The reproductive cycle is very short. In particular, at a seawater temperature of 13 °C, the average duration of a generation is 9.5 days (Paffenhöfer, 1973), and this decreases to 5–6 days at 15 °C (Thompson et al., 2001) and 3–5 days at 20–22 °C (Fenaux, 1976). Sexual maturation is very rapid since, at 15–20 °C, gonad appearance begins from day 1 after metamorphosis, sexual differentiation and gonad development occur within days 3–4, and maturity and spawning are complete within days 5–6 (Nishino and Morisawa, 1998; Ganot et al., 2006; Nishida, 2008; Danks et al., 2013). This species is the appendicularian most widely studied by ecologists and developmental biologists, and recently, it has risen to model organism after the achievement of a browser resource (http://oikoarrays.biology.uiowa.edu/Oiko/) for its genome and developmental transcriptome (Danks et al., 2013). As an adaptation to its particular lifestyle, its genome is smaller than that of other tunicates, being only 70 Mbp (Cañestro et al., 2007; Denoeud et al., 2010), and corresponds to the massive loss and remodelling of genes demonstrated by whole genome analysis (Satoh, 2016).

E-mail address: francesca.cima@unipd.it.

https://doi.org/10.1016/j.ydbio.2018.09.004
Received 25 May 2018; Received in revised form 2 August 2018; Accepted 5 September 2018
Available online 10 September 2018
0012-1606/

After metamorphosis, during the growth of individuals, the somatic cell lineages, although increasing in size, remain eutelic, i.e., fixed in number, with an absence of regeneration capability (Martini, 1909; Meinertzhagen, 2005), whereas the number of cells in the germ line increases. *O. dioica* is the only gonochoric species in the class Appendicularia, which includes proterandric hermaphroditic species in which the gonad primordium, namely, the 'ovotestis' (Bolles Lee, 1884; Fenaux, 1967), appears soon after metamorphosis and then divides into two structures, testis and ovary, in the post-abdominal region of the trunk posteriorly to the digestive tract. In *O. dioica*, the gonad (testis or ovary) develops posteriorly to the gastric lobes inside the genital cavity, the latter of which is delimited by both the epidermis and the gut wall, and gradually surrounds part of the digestive tract. The morphology of the testis is formed of two cell types, i.e., the cells of the germ line and the accessory or somatic cells, the latter forming the thin wall of the testis. At the end of testis development, a short spermiduct appears (Fenaux, 1976; Galt and Fenaux, 1990) together with a gonad-specific structure, the 'moustache', present in both male and female individuals, that opens the gonad epithelium when gametes are mature for their release into the environment, causing individual death (Ganot et al., 2006). In hermaphroditic species, to avoid self-fertilisation, sperm spawning occurs approximately 30 min before that of eggs (Fenaux and Gorsky, 1983). Sperm spawning does not occur during the activity of water filtering of an animal surrounded by its bubble-shaped house; otherwise, the sperm might be captured by the house filters together with the food particles. This hypothesis is confirmed by the observation that reared individuals of *Oikopleura longicauda* during their gamete spawning are free swimming without their house (Fenaux and Gorsky, 1983). When the gametes, which have a haploid chromosomal pool with 8 chromosomes (Colombera and Fenaux, 1973), are released into the seawater, they can unite immediately after spawning but can also remain viable for 24 h (Galt, 1972).

The correlative events of spermatogenesis and testis development in tunicates have been studied by a few authors (Franzén, 1983; Burighel and Martinucci, 2000). Most observations on spermatogenesis have been reported for ascidians (Grier, 1992; Cavey, 1994) and thaliaceans (Holland, 1988, 1989, 1990), which show asynchronous spermatogenesis, where the same testis shows clusters of cells at different spermatogenetic stages (Burighel and Cloney, 1997; Godeaux et al., 1998), but studies on appendicularians are few and restricted to hermaphroditic oikopleurids (Bolles Lee, 1884; Fenaux, 1963, 1967; Galt and Fenaux, 1990; Ganot et al., 2006; Savelieva and Dautov, 2012), and fritillarids (Salensky, 1904; Martinucci et al., 2005). Appendicularians have synchronous spermatogenesis (Salensky, 1904; Burighel and Martinucci, 2000). This synchronisation, pivotal to ensure the fertilisation of the low amount of eggs spawned in the pelagic environment, occurs due to the formation of complex syncytial structures inside the whole testis, which connect all the germ cells at the same differentiation stage through cytoplasmic bridges from which gametes begin to detach only in the late stages of spermatogenesis as spermatids.

Knowledge of the sperm morphology of appendicularians is also very scant. Only in *O. dioica*, the structure of the mature spermatozoon and its behaviour during egg fertilisation have been described (Flood and Afzelius, 1978; Holland et al., 1988). The mature spermatozoon of this species is very small in comparison with that of the other tunicate classes and is not of the 'ascidiosperm' type (Jamieson, 1991), which possesses i) an elongated, rod-like nucleus, ii) an acrosome reduced to small vesicle(s) or absent, iii) a single mitochondrion flanking the nucleus, and iv) a tail represented by flagellum emerging from the distal centriole, which constitutes the basal body. Appendicularians have a primitive spermatozoon (Franzén, 1970) with i) a globular head with a large acrosome and ii) a mid-piece with a mitochondrion that surrounds the axoneme. As another difference from other tunicates with external fertilisation, this spermatozoon undergoes a reaction leading to the formation of an acrosomal process (Holland et al., 1988; Burighel and Martinucci, 2000), similar to the well-known in sea urchins.

To provide more insight into the spermatogenesis of appendicularians, changes in shape, size and colour of the testis of *O. dioica*, which currently represent a unique way for rapidly staging individuals (Fenaux, 1963, 1967; Shiga, 1976), have been examined during individual growth considering the relationships between the gross morphology of the testis and the events of sperm differentiation. As a difference of previous ultrastructural studies limited to description of mature spermatozoon (Flood and Afzelius, 1978) and synthetic comparison with fritillarids (Martinucci et al., 2005), a staging of testis development based on histological analysis is proposed. For the richness of anatomical and histological details, it appears more careful than that based on days after metamorphosis, the latter currently used by many authors for molecular studies but imprecise and depending on temperature and other factors, such as the presence of nutrients, physical injuries, and population density. It can also contribute to improve future knowledge on the biology and lifecycle of these organisms in light of phylogenesis and evolutionary history.

2. Materials and methods

Some of the 50 individuals of *O. dioica* used in the present study were collected in the bay of Villefranche-sur-Mer (France) with plankton nets (200-μm mesh) in spring, autumn and winter, whereas other individuals were directly obtained from larvacean rearing at the Station Zoologique, CEROV. Since *O. dioica* is a few millimetres long (approximately 1 mm for the trunk and 4 mm for the tail) and lives in a gelatinous house, from which it escapes quickly when disturbed, animals were made to abandon their houses by touching them with a sharp needle before fixation. Whole animals were immediately fixed in a solution of 1.5% glutaraldehyde in 0.2 M cacodylate buffer, pH 7.4, plus 1.6% NaCl, for 2 h and then rinsed in cacodylate buffer containing 1.6% NaCl. They were post-fixed in 1.5% OsO_4 in cacodylate buffer, dehydrated, and embedded in Epon 812 (Fluka) for sectioning.

The maturity stage of the testis was determined in the first approximation considering for each individual the size of both the trunk and gonad. The testis of selected individuals, previously observed and photographed *in toto* under a Leica MZ6 stereomicroscope equipped with a DV Leica EC4 and the Leica Application Suite version 3.2.0. (Leica Microsystems Limited 2015), were completely dissected to check both the differentiation stage and the development of the germ cells inside the gonad. Individuals were successively assigned to a specific maturity stage as follows: 4 individuals to stage 1 and 2 (proliferative phases), 8 individuals to stage 3 (pre-meiotic phase), 11 individuals to stage 4 (meiotic phase), 28 individuals to stages 5, 6, 7 (spermiogenesis).

For a detailed reconstruction of the gonad, sections of individuals at the same developmental stage were made serially in different planes with an LKB ultramicrotome. The sections (1 μm thick) were hot stained with toluidine blue and observed with an Olympus CX31 light microscope (LM) equipped with a DV Lumenera Infinity 2 and Infinity Capture Application software version 5.0.0 (Lumenera Co. 2002–2009). Ultrathin sections (60 nm thick) were collected on copper grids, stained with uranyl acetate and lead citrate and then examined under an FEI TECNAI transmission electron microscope (TEM) equipped with a TIETZ high-resolution digital camera at 75 kV.

3. Results

Seven developmental stages of the testis were established after observations under a stereomicroscope of numerous individuals *in toto*. The relationships between the anatomy and cytology of the various stages of testis development have been determined with seriated sections of embedded specimens and their relative histological observations under LM and TEM. For the characterisation of the

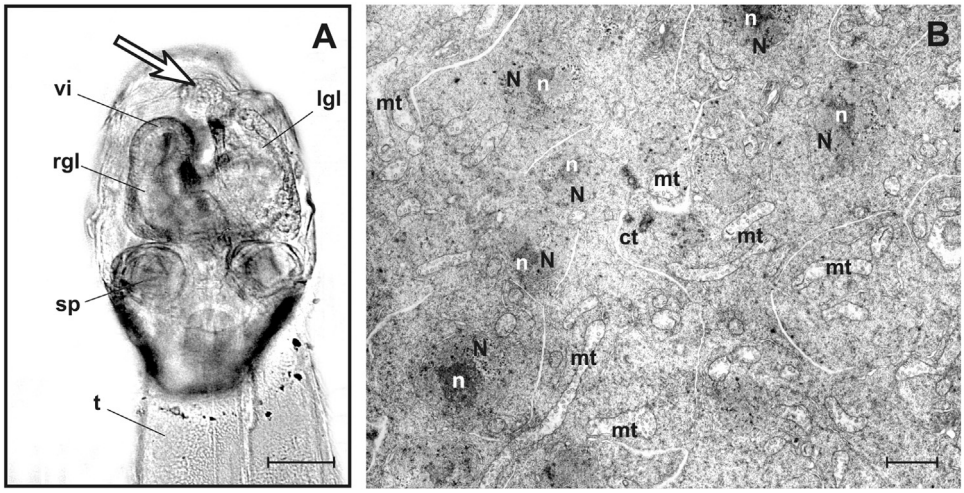

Fig. 1. Stage 1. (A) Specimen *in toto* of *Oikopleura dioica* showing the dorsal side of the trunk with the proximal part of the tail. Note the gonad primordium (arrow) in the genital cavity. (B) Gonad at TEM. Gonocytes appears as undifferentiated cells showing a large nucleus with an electron-dense nucleolus, and a cytoplasm rich in ribosomes and mitochondria. ct: centriole, lgl: left gastric lobe; mt: mitochondrion; N: nucleus; n: nucleolus; rgl: right gastric lobe; sp: spiracle; t: tail; vi: vertical intestine. Scale bars: A = 30 μm; B = 1 μm.

differentiation stages of spermatogenesis, the following elements were principally considered: shape and size of testis related to the trunk length and the posterior part of the alimentary canal, germ-cell size and their relationships with the syncytium, nuclear chromatin arrangement, flagellum appearance, presence and position of large mitochondria, acrosome assembly and changes in the Golgi complex.

3.1. Stage 1: Early proliferative phase

The first differentiation stage is represented by a small spherical rudiment of the gonad that is recognisable in individuals of small size, i.e., with a trunk length of approximately 0.4 mm. This transparent primordium is placed in the genital or gonad cavity - which is just slightly developed - posteriorly to the gastric lobes. At this stage, the gonad is undifferentiated, and the simple observation of specimens *in toto* or of sections under LM did not allow us to establish whether the primordium belongs to an ovary or a testis (Fig. 1A). It is covered by a thin and flattened single-layer epithelium of somatic cells separated by epidermis, whereas internally, it is completely engaged by undifferentiated proliferating 'gonocytes' ultrastructurally indistinguishable between male or female germ cells, which appear supplied with a large nucleus and an evident nucleolus (Fig. 1B).

3.2. Stage 2: Late proliferative phase

At this stage, the gonad is ovoidal in lateral view (Fig. 2A) and lengthened dorsally in the genital cavity, where it appears U-bent with its two extremities widening to contact anteriorly both the gastric lobes and the vertical intestine (Fig. 2B) and its convexity expanding postero-dorsally to contact the epidermis with the somatic cells of the epithelial wall (Fig. 2C). Under TEM, the male gonocytes are ovoidal in shape ('spermatogonia') and closely leaned each other. The cell boundaries are not always well distinguishable, and cells appear in contact with each other inside a germ-line syncytium (Fig. 2D). The nucleus of spermatogonia is roundish, with granular, scattered chromatin and may contain a nucleolus. The abundant cytoplasm is rich in ribosomes, often organised to form polysomes. Both the smooth and the rough endoplasmic reticula are scarcely represented. Some cells show centrioles in a duplication phase. Mitochondria, scattered in the cytoplasm, are not abundant, assume various shapes, i.e., roundish or rod-like, and have a few cristae mainly located at the periphery of the clear matrix. The Golgi complex is slightly developed and characterised by a few cisternae and peripheral vesicles (Fig. 2E). The somatic cells of the wall appear flattened and in contact with each other through latero-apical junctions, which can be very long (inset of Fig. 2D). These junctions are a constant feature and, for their position, clearly separate the apical compartment from the baso-lateral one. Between the germ cells and the epithelial cells, a thin space remains, but in some areas, the two cell types contact each other through tight junctions marked by electron-dense material.

3.3. Stage 3: Pre-meiotic phase

The gonad is increased in size and bends antero-dorsally, forming a protrusion reducing the genital cavity and increasing the contact surface with the stomach, particularly with its right lobe. Laterally, the gonad appears cup-shaped and dorsally shows a large depression dividing it into two symmetrical parts (Fig. 3A). Under TEM, the germ cells still appear like undifferentiated cells (Fig. 3B) but show characteristics typical of a predisposition to begin meiosis ('primary spermatocytes'). They are indeed larger than the germ cells of stages 1–2, with an increased nucleus/cytoplasm ratio. The nucleus occupies most of the cell volume, its chromatin begins to condense in clusters at the periphery, and the nucleolus disappears. In the cytoplasm, numerous ribosomes are present, and duplicating centrioles are frequently found. Overall, a very extensive, syncytial structure spreads out the most of the testis volume. From this structure, some germ cells hang as a grape bunch, whereas other ones seem to be isolated (Fig. 3C). Inside the common cytoplasmic structure, numerous mitochondria appear large and various in shape. Other smaller mitochondria are located in the cytoplasmic branches and separate together with the germ cells. The Golgi complex is scarcely developed and located near the mitochondria.

3.4. Stage 4: Meiotic phase

Below the dorsal protrusion of the testis, another smaller, digitiform one appears, which partially threads between the two gastric lobes and is recognisable laterally in the genital cavity. The two symmetrical parts of the gonad described in stage 3 are now increased in an asymmetrical way (Fig. 4A), the right one being more lengthened and surrounding laterally and ventrally the right lobe of the stomach. The form of the gonad is concave and, in transverse section, is typically ring-shaped for the presence of a central cavity (Fig. 4B), where diaphanous, myelin-like structures and cell debris are recognisable (Fig. 4C). The syncytial structure persists and acquires a more ramified feature than in the previous stages because the cytoplasmic branches grow longer and thinner and extend inside a great part of the testis. The

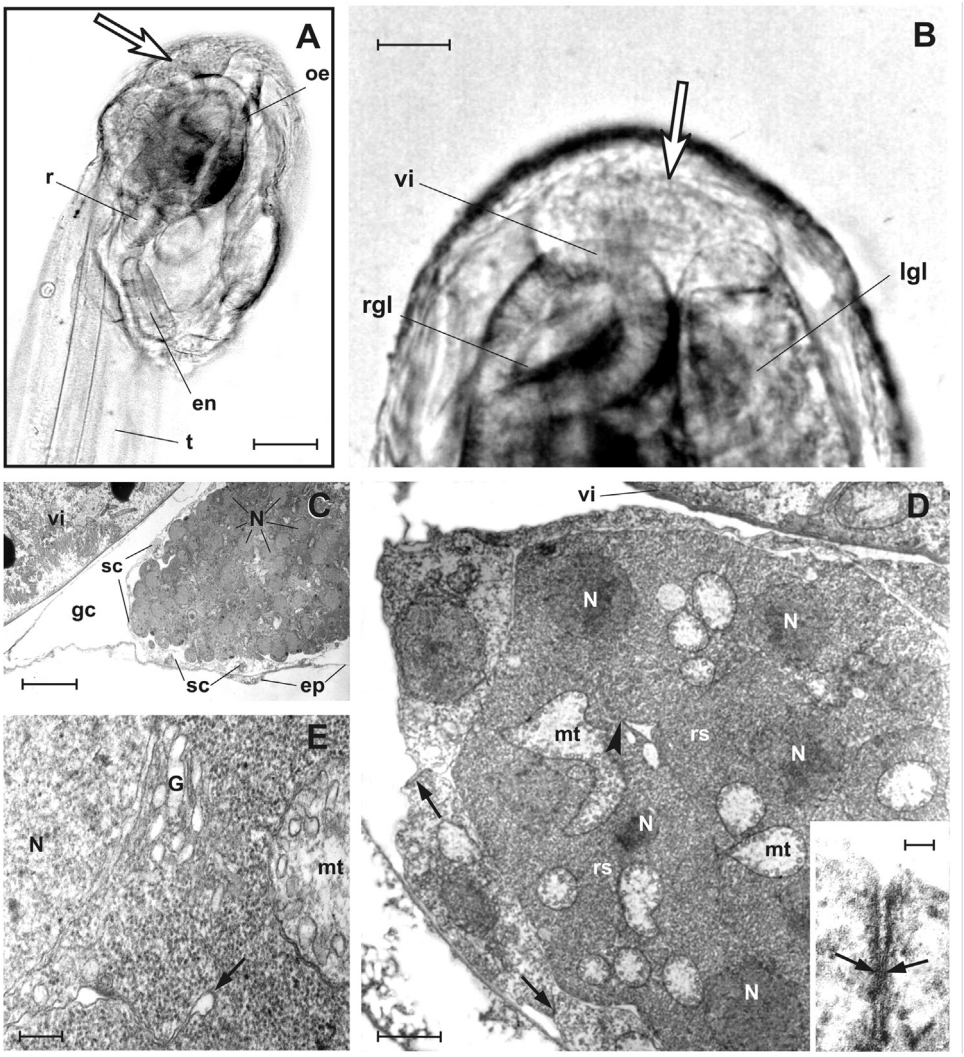

Fig. 2. Stage 2. (A, B) Specimens *in toto* of *Oikopleura dioica* showing the dorsolateral side of the trunk with the proximal part of the tail (A), and the posterior part of the trunk, viewed dorsally (B), with detail of the genital cavity and testis (arrow). (C-E) Gonad at TEM. (C) Frontal section of the testis located in the genital cavity next to vertical intestine. Germ cells entirely occupy the testis, the nuclei of which are recognisable. At the periphery, the thin layer of somatic cells of the testis wall is well separated from the epidermis. (D) The somatic cells of the wall are flattened and joined together by brief apicolateral junctions (arrows), which appear of tight type due to the presence of electron-dense contact points between the opposing membranes (inset of D). Germ cells are spermatogonia separated partially by plasma membrane (arrowhead in D and arrow in E). (E) A Golgi complex with scanty cisternae and vesicles is close to the nucleus. en: endostyle; ep: epidermis; G: Golgi complex; gc: genital cavity; lgl: left gastric lobe; mt: mitochondrion; N: nucleus; oe: oesophagus; r: rectum; rgl: right gastric lobe; rs: ribosomes; sc: somatic cells; t: tail; vi: vertical intestine. Scale bars: A = 60 μm; B = 24 μm; C = 4 μm; D = 1.6 μm; inset in D = 54 nm; E = 0.25 μm.

germ cells hanging from this structure through cytoplasmic bridges appear to be more isolated than in the previous stages, and the intercellular spaces are much wider. These joining bridges are ring-shaped and marked by an electron-dense layer of F-actin that internally covers the plasma membrane. Through these communications, it is possible that exchanges of cytoplasmic material and organelles, particularly of mitochondria, occur (Fig. 4D). The germ cells are 'secondary spermatocytes' (Fig. 4E). Their nucleus, indeed, displays a highly homogeneous aspect, with the exception of evident peripheral clusters of chromatin, and is characterised by the presence of synaptonemal complexes formed by the pairing of the homologous chromosomes during the meiotic prophase. They are located at the nuclear periphery because the presence of the nuclear membrane is necessary for chromosomal pairing. The cytoplasm is further reduced. Mitochondria increase in number and are located mainly inside the syncytial structure. They are polymorphous and occasionally narrowed; their cristae appear tubular and/or laminar and are distribute not only at the periphery, as previously described in stage 2, but in the whole matrix. Near the nucleus, the Golgi complex is visible and is represented by a few flattened cisternae. All spermatocytes display two centrioles in a duplication phase, located always in opposite cytoplasmic position with respect to the area connecting syncytium (Fig. 4D).

3.5. Stage 5: Early spermiogenesis

The trunk grows longer (0.8–1 mm) due to the volumetric increase of the genital cavity. As regards the testis, at this stage the digitiform median protrusion and ventral wrapping of the right gastric lobe become more evident, reaching their maximum size (Fig. 5A). At LM, the sections show numerous germ cells in close proximity to each other and with dark blue nuclei. Under TEM, they can be identified as 'post-meiotic spermatids'. The first aspect that characterises the 'early spermatids' when they are still attached to syncytium is the process of flagellum formation from the distal centriole, whereas the proximal centriole tends to regress (Fig. 5B). The lengthening of the flagellum, with the typical 9 + 2 axonemal pattern, begins from the posterior extremity of the spermatid and involves a change in the shape of the germ cell, the latter appearing longer than a spermatocyte at stage 4. The nucleus maintains an ovoidal form and contains homogeneous chromatin. The cytoplasm is rich in ribosomes. The syncytial structure

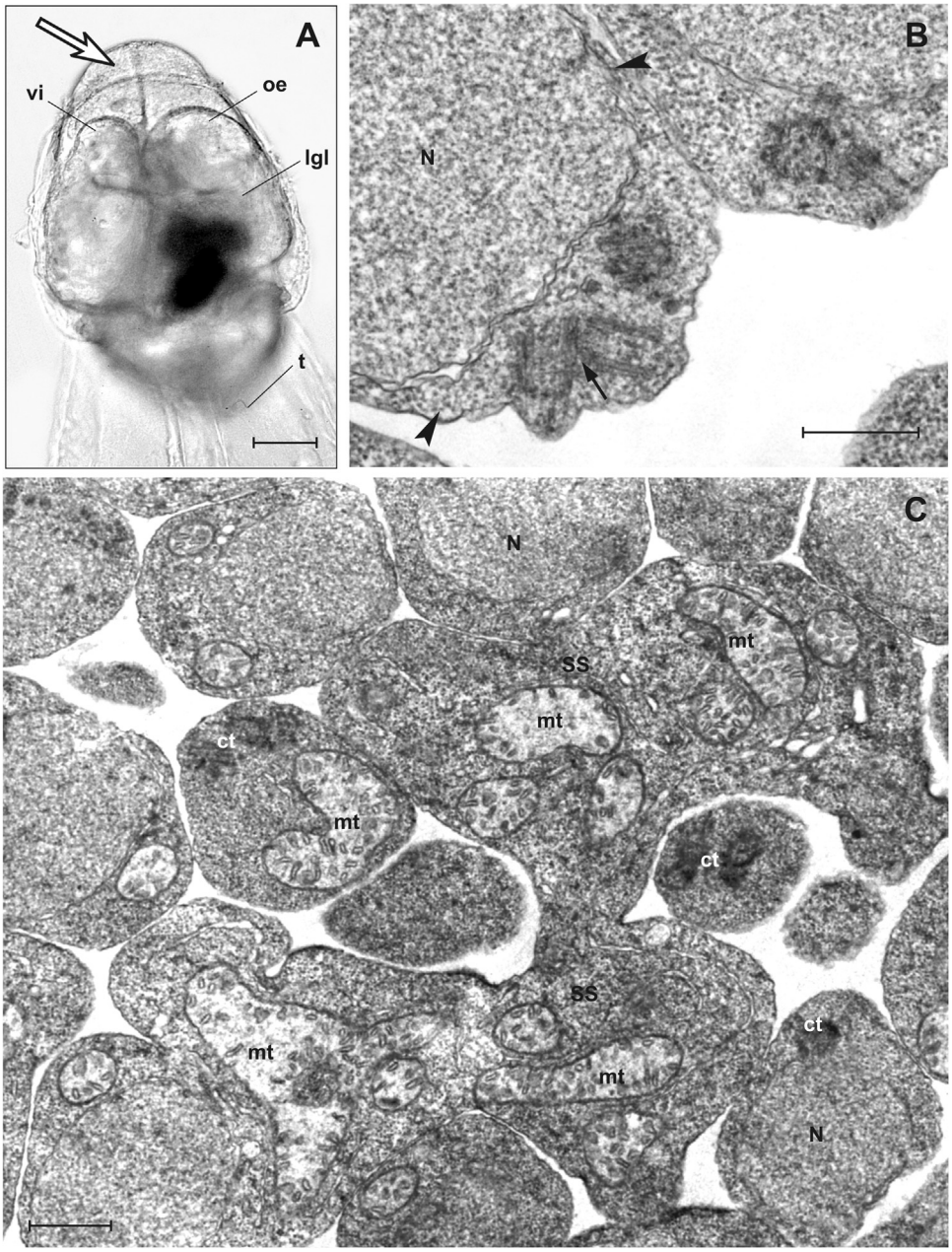

Fig. 3. Stage 3. (A) Specimen *in toto* of *Oikopleura dioica* showing the dorsal side of the trunk with the proximal part of the tail and, posteriorly, the genital cavity with the testis (arrow). (B) Detail of primary spermatocytes with nuclei showing homogeneous chromatin and surrounded by a thin cytoplasmic strip (arrowheads). A pair of centrioles (arrow) is duplicating. (C) Numerous primary spermatocytes are interconnected through syncytial structures. The nucleus occupies most of the cytoplasm and centrioles are duplicating. Mitochondria of the syncytial structure are voluminous and polymorphic, whereas those inside isolated spermatogonia are smaller. ct: centriole; lgl: left gastric lobe; mt: mitochondrion; N: nucleus; oe: oesophagus; SS: syncytial structure, t: tail; vi: vertical intestine. Scale bars: A: 67 μm; B = 0.5 μm; C = 0.6 μm.

is still present and branched, although the number of isolate spermatids is increased (Fig. 5C). Some of the mitochondria begin to migrate laterally next to the nucleus of the spermatids, although most of them remain in the syncytial structure together with the Golgi complex and numerous cisternae of the endoplasmic reticulum. It is noteworthy the different trends of the mitochondria in bending and closing inside the spermatids and melting in a large, lobed mitochondrial mass inside the syncytial structure.

As spermiogenesis continues, the 'intermediate spermatids' are characterised by the process of acrosome formation (Fig. 5D–F). They are globular in shape, with a straight, long flagellum and appear distributed free in the most part of the testis volume, with large spaces between them but with an intercellular bridge of 0.4 μm of diameter linking them to the syncytial cytoplasmic structure. The nucleus, with an average diameter of 0.9 μm, has two small channels raised from membrane inpocketing at its opposite poles, where the acrosome and the basal body of the flagellum, respectively, insert. The chromatin appears homogeneous but more condensed than at early stage 5. The mitochondrion is large, positioned laterally to the nucleus, and occasionally, its passage across the intercellular bridges from the mitochondrial mass of the syncytium is recognisable. The acrosome is developing and is formed of 6–7 vesicles, ranging from 80 to 160 nm in diameter and with strongly electron-dense contents. Some of these vesicles are placed in a small anterior channel of the karyotheca, which has the two nuclear membranes adhering to each other, whereas other vesicles are still scattered in the cytoplasm near the Golgi complex formed of 3–4 stacked cisternae (Fig. 5E). At the nuclear apex, between the electron-dense vesicles, the external

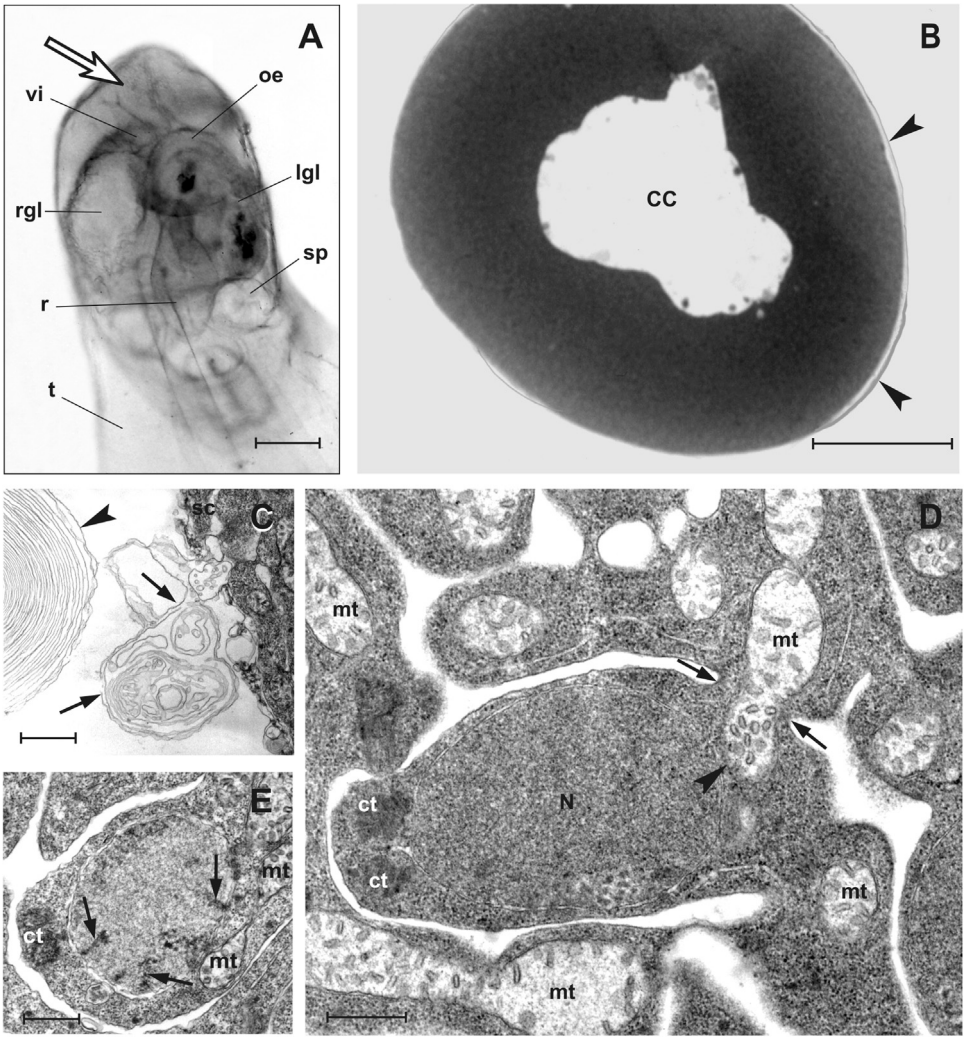

Fig. 4. Stage 4. (A) Specimen *in toto* of *Oikopleura dioica* showing the dorsal side of the trunk with the proximal part of the tail and, posteriorly, the genital cavity with the testis (arrow). (B) Transverse thick section of the testis stained with toluidine blue. A thin wall of somatic cells (arrowheads) is visible at the periphery. Note the presence of a central cavity. (C) Details at TEM of the central cavity also delimited by somatic cells of the wall, where numerous remnants of membranes are present, some of which detach from these cells (arrows) and show a myelin-type arrangement of the membranes (arrowhead). (D) Detail of a secondary spermatocyte with duplicating centrioles on the opposite side of the connecting bridge (arrows) with the syncytial structure. Note the passing of a mitochondrion from the syncytial structure to the spermatocyte through the bridge (arrowhead). (E) Detail of a secondary spermatocyte showing the presence of synaptonemal complexes (arrows) that adhere to the nuclear membrane, and duplicating centrioles in the cytoplasm. CC: central cavity; ct: centriole; lgl: left gastric lobe; mt: mitochondrion; N: nucleus; oe: oesophagus; r: rectum; rgl: right gastric lobe; sc: somatic cells; sp: spiracle; t: tail; vi: vertical intestine. Scale bars: A: 76 μm; B = 170 μm; C = 1 μm; D, E = 0.5 μm.

nuclear membrane forms a digitiform evagination 200 nm long and 40 nm wide that contains clear material and is anchored to the electron-dense vesicles by fibrillar material (Fig. 5F). On the posterior side of the nucleus, the basal body of the flagellum is partially placed in a channel 0.1 μm in length and partially in the cytoplasm.

3.6. Stage 6: Late spermiogenesis

The testis is completely developed and fills the genital cavity (Fig. 6A). It has a fibrous aspect, and germ cells occupy the whole volume of the gonad. Under LM, the germ cells seem to be in a very advanced stage of spermatogenesis because most of them are isolated and show very distinguishable head and tail. Under TEM, spermatid segregation is almost complete, the syncytial structures are reduced, and their cytoplasm appears to be empty of both mitochondria and cisternae of the Golgi complex (Fig. 6B). The 'late spermatids' (Fig. 6C–D) are tadpole-shaped with i) a lengthened head containing the nucleus, the acrosome and the basal body of the flagellum, ii) the mid-piece containing the only mitochondrion surrounding the proximal part of the flagellum, and iii) the tail formed of the free portion of the flagellum. The nucleus, which is very reduced in size due to the elimination of a lot of the nucleosome, is ring-shaped and not perforated at its centre because of the presence of an isthmus surrounded by the nuclear membrane. In the nucleus, two regions are well recognisable, i.e., i) an anterior channel (360 nm × 200 nm), where the acrosome is placed, and ii) a posterior channel (400 nm × 200 nm), which contains the basal body and the proximal portion of the flagellum. The chromatin appears condensed, showing a scattered feature organised into electron-dense plaques with a thin clear space along the nuclear membrane. The cytoplasm is still abundant and rich in ribosomes, vesicles and cisternae of the Golgi complex. Only one mitochondrion is present, which is not very lengthened, contains tubular and laminar cristae, and is placed laterally to the nucleus (Fig. 6C) or, more frequently, in the mid-piece behind the nucleus (Fig. 6D), wrapping the axoneme of the flagellum and bending as a C when observed in transverse section. The acrosome is cylindrical and measures 320 nm × 180 nm, and its axis is little slanting in comparison

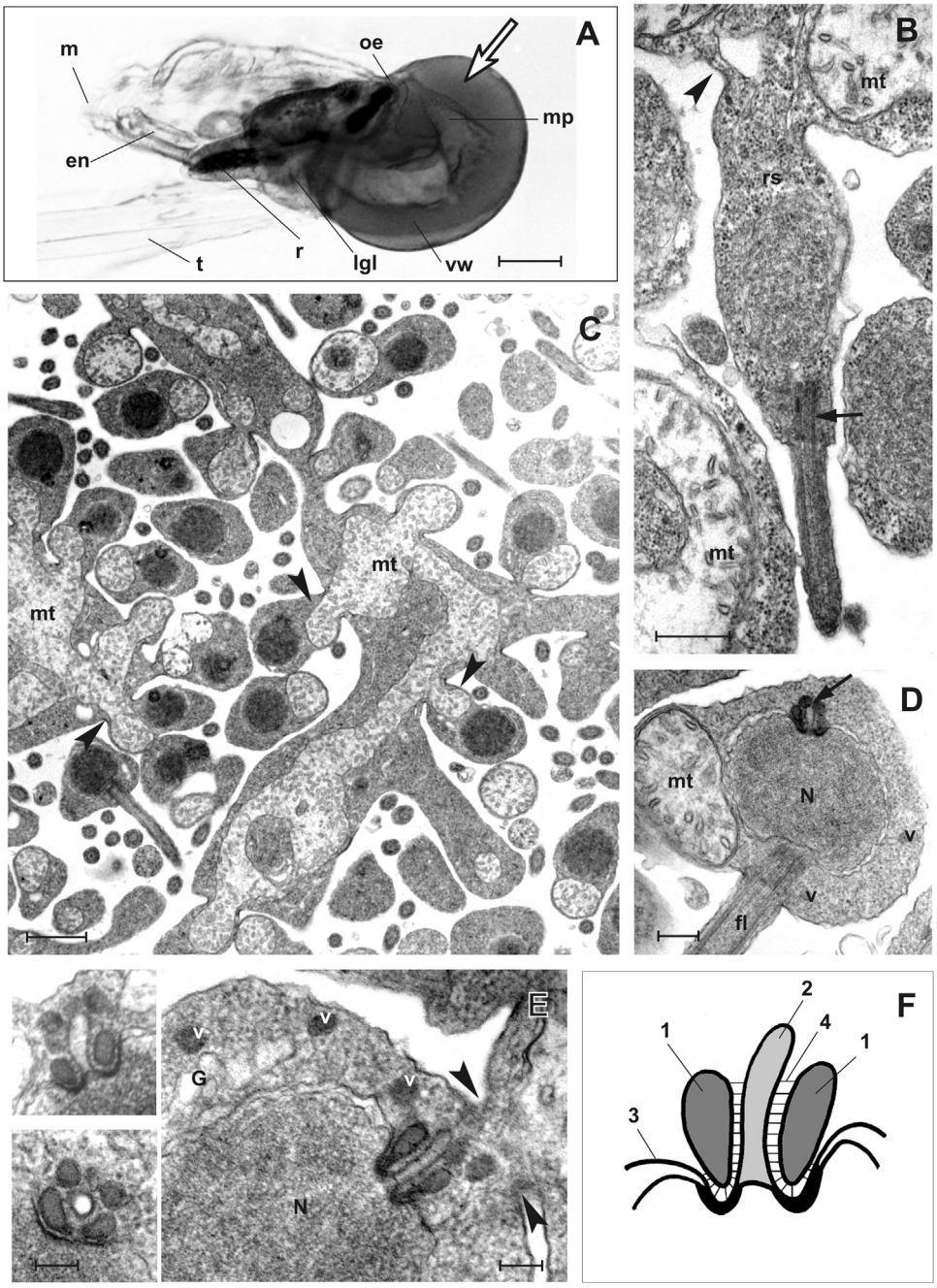

Fig. 5. Stage 5. (A) Specimen *in toto* of *Oikopleura dioica* showing the left side of the trunk with the proximal part of the tail and, posteriorly, the genital cavity with the testis (arrow). (B) Early spermatid under TEM. The flagellum is growing from the distal centriole (arrow). The cell is in cytoplasmic relationships with the syncytial structure (arrowhead). (C) Portion of the testis with numerous intermediate spermatids still attached to the syncytium through cytoplasmic bridges. A large mass of mitochondria is present in the common cytoplasm and extends its portions inside spermatids (arrowheads). Spermatids contain a roundish nucleus, the flagellum, the acrosome, and the lateral mitochondrion. (D) Intermediate spermatid with the mitochondrion on one side of the subspherical nucleus. The acrosome (arrow) is formed by 6–7 dense vesicles, of which 4 are visible, around a clear evagination of the outer nuclear membrane. Other vesicles are scattered in the cytoplasm near the Golgi complex. The basal body is just embedded in the posterior part of the nucleus and continues with the intracytoplasmic and free portions of the flagellum. (E) The cytoplasmic bridge that connects the intermediate spermatid to the syncytium is still present (arrowheads). The organising acrosome throughout various planes (longitudinal on the top, transverse on the bottom) is reported in detail (insets of E). (F) Sketch of a longitudinal section of the acrosomal zone. Four electron-dense vesicles, two of which (1) are visible, are arranged around a clear central evagination (2) of the outer nuclear membrane (3) anchored by protein fibrous material (4). ct: centriole; en: endostyle; fl: flagellum; G: Golgi complex; lgl: left gastric lobe; m: mouth; mp: digitiform median protrusion of testis; mt: mitochondrion; N: nucleus; oe: oesophagus; r: rectum; rs: ribosomes; v- vesicle; vw: ventral wrapping of gastric lobes by testis; t: tail. Scale bars: A = 100 μm; B = 0.5 μm; C = 1.12 μm; D = 0.26 μm; E and insets = 80 nm.

with the principal axis of the cell. It arises from the fusion of the vesicles with electron-dense contents, observed in stage 5, in one vesicle surrounding the central vesicle, which is cone-shaped and with clear contents (insets of Fig. 6C). Both nuclear membranes adhere to each other around the acrosome, and in the basal portion of the acrosome, they form a socket in which finely granular material can be recognised.

3.7. Stage 7: Completion of sperm differentiation and release

This is the stage of full maturity of the testis, which reaches its maximum extent (Fig. 7A) and is characterised by the appearance of a short spermiduct in the median-dorsal position (Fig. 7B). Across this duct and the moustache, the emptying of the male gonad occurs through the spawning of the functional sperm in the sea water. This

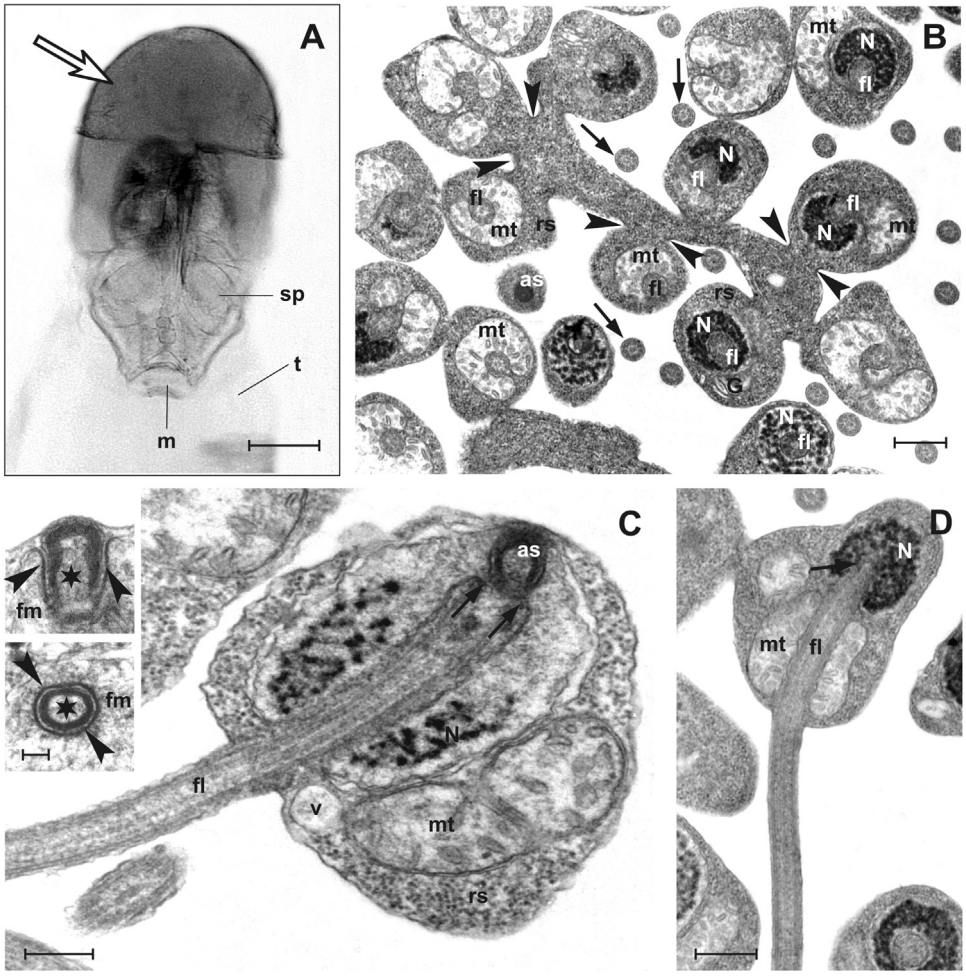

Fig. 6. Stage 6. (A) Specimen *in toto* of *Oikopleura dioica* showing the dorsal side of the trunk with the proximal part of the tail and, posteriorly, the genital cavity with the testis (arrow). (B) Syncytial structure under TEM, from which the spermatids appear to bud staying connected to the thickened plasma membrane with short cytoplasmic bridges (arrowheads). The mitochondrion is large and surrounds the spermatid flagellum. (C, D) Longitudinal sections of the head of a late spermatid showing the relationships between the nucleus, the flagellum and the acrosome. In the nucleus, chromatin is organised and condensed into thick plaques. The flagellum and the acrosome penetrate the posterior nuclear channel (arrow in D) and the anterior nuclear channel, respectively, and remain separate from the nuclear membrane (arrows in C). Mitochondrion flanks both flagellum and nucleus. In insets of (C), longitudinal (on the top) and transverse (on the bottom) sections of the acrosome show diffuse fibrogranular material in the nuclear portion close to the anterior channel, the inner clear region (asterisk), and the two nuclear membranes (arrowheads) bounding the anterior channel as: acrosome; fl: flagellum; fm: fibrogranular material; G: Golgi complex; m: mouth; mt: mitochondrion; N: nucleus; rs: ribosomes; sp: spiracle; t: tail; v: vesicle. Scale bars: A: 140 μm; B = 0.5 μm; C = 0.2 μm; insets in C = 0.1 μm; D = 0.4 μm.

process is very fast (approximately 20 min), so it is difficult to find specimens at this stage. The necessary manipulations for the capture of mature specimens often provokes the break of the body wall and the discharge of the spermatozoa. Under TEM, the cytoplasmic syncytium disappears, and the spermatozoa completely separate from each other, fill up the testis and are surrounded by the flattened cells of the testis wall (Fig. 7C). In the mature sperm ('spermatozoon'), the three regions of head, mid-piece and tail are clearly distinguishable (Fig. 5D). In comparison with the previous stage, the head of the spermatozoon is more lengthened and narrower due to the reduction in the cytoplasm around a roundish nucleus, approximately 1 μm long and 0.6 μm wide, with homogeneously condensed chromatin; fibrogranular material is still recognisable close to the anterior nuclear channel. Small vesicles can be found scattered in the cytoplasm, mainly near the nucleus. The acrosome (Fig. 5E) is ovoidal and completely developed (320 nm × 180 nm) and is slanting in comparison with the longitudinal axis of the head. The posterior portion of the acrosome has a socket, where the nuclear membranes of the anterior nuclear channel insert and appear closely adhering each other. The central cone of the acrosome is formed of less electron-dense and more filamentous material than in the previous stage. In some longitudinal sections, at the apex of the acrosome, the membrane is extended to form a vesicle that is melted with the plasma membrane (inset of Fig. 5D). In the central zone, the nucleus forms the posterior nuclear channel for implantation of the flagellum, which further extends in this channel, reaching a length of 700 nm, i.e., almost the entire length of the nucleus. In the mid-piece, the mitochondrion is placed behind the nucleus surrounding the axoneme, and its morphology is changed in comparison with the previous stages because it displays a more lengthened form (approximately 2 μm long and from 0.5 to 1 μm wide) and has laminar cristae and granular material in its matrix. The tail, formed of the 26-μm long free portion of the flagellum, has an axoneme with the typical 9 + 2 pattern of microtubule doublets, and the distal centriole constitutes the basal body of the flagellum showing the usual 9 + 0 pattern of microtubule triplets.

4. Discussion

In a recent study of the entire morphology of adult of the model appendicularian *O. dioica*, scanning electron microscopy (SEM) and 3D images were used to categorise spermatogenesis as in the early (meiotic phase), intermediate (post-meiotic phase) and late (spermatozoon formation) stages, each separated by approximately 4-h periods (Onuma et al., 2017). However, the size of the gonad does not

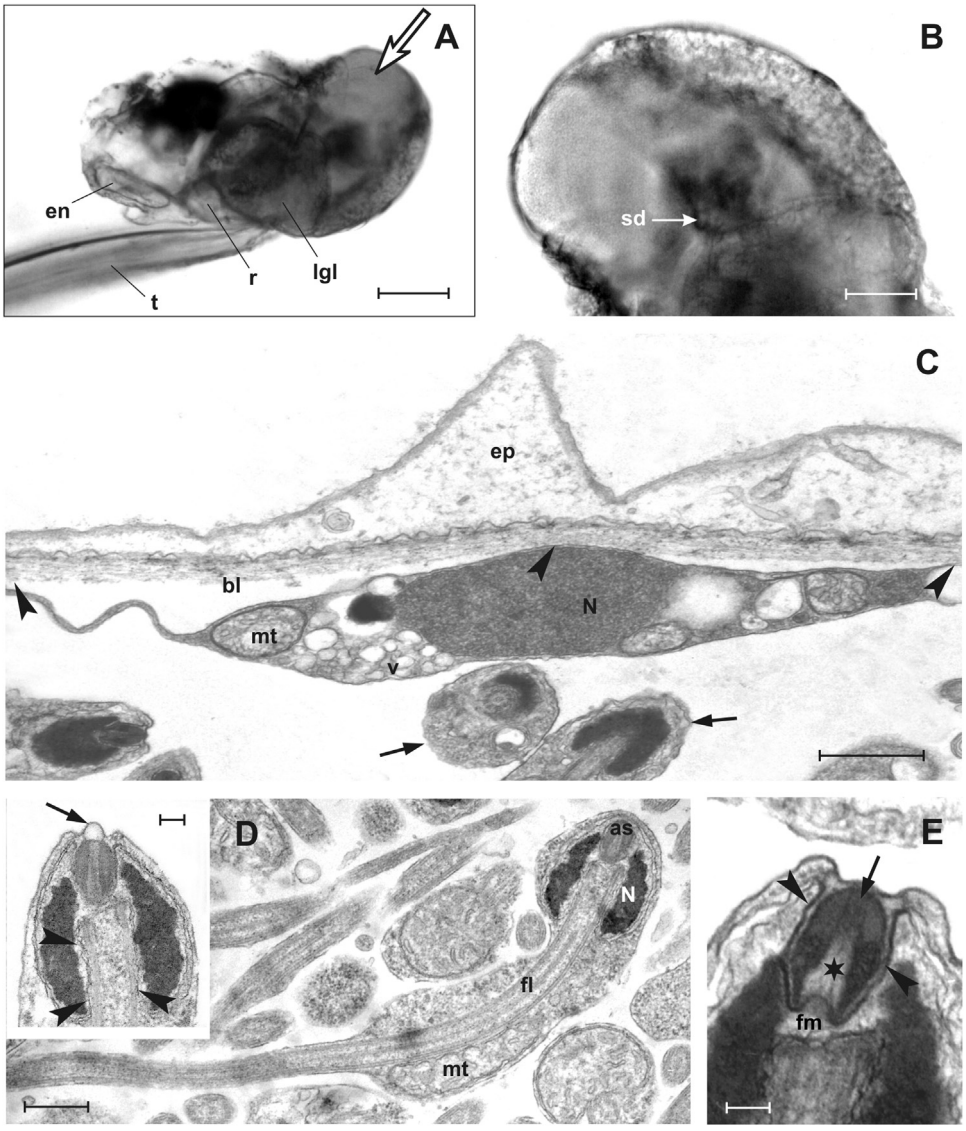

Fig. 7. Stage 7. (A) Specimen *in toto* of *Oikopleura dioica* showing the left side of the trunk with the proximal part of the tail and, posteriorly, the genital cavity with the testis (arrow). (B) Dorsal view of the testis showing the median short spermiduct (see Fig. 1a in Ganot et al., 2006 for a reference photo of the moment of sperm ejection). (C) Spermatozoa (arrows) near the testis wall formed by very flattened cells that lean at some points against the basal lamina of the epidermis (arrowheads). (D, E) Mature spermatozoon sectioned longitudinally. The nucleus consists of condensed chromatin. The mitochondrion is elongated and enveloping much of the flagellum behind the head and forms the mid-piece. The acrosome (arrow in E) is enveloped by the nuclear membrane (arrowheads in E) and is crossed by a clear wedge-shaped region (asterisk in E). Occasionally, a small clear vesicle overlaps the acrosome and merges with the plasma membrane (arrow in inset of D). The proximal part of the flagellum continues to be held in the posterior nuclear channel (arrowheads in inset of D). as: acrosome; bl: basal lamina; en: endostyle; ep: epidermis; fl: flagellum; fm: fibrogranular material; lgl: left gastric lobe; mt: mitochondrion; N: nucleus; r: rectum; sp: spermiduct; t: tail; v: vesicle. Scale bars: A = 150 μm; B = 70 μm; C = 1.5 μm; D = 0.4 μm; inset in D = 0.1 μm; E = 0.1 μm.

represent a good criterion to establish beforehand the differentiation degree of the testis. In the present study, the first difficulty arose at the moment of choosing specimens with gonads at various differentiation stages only on the basis of observations *in toto*. To characterise the differentiation of the testis, a comparison between the gross morphology of the testis with parallel observations of sections under a LM and TEM was performed on numerous individuals. Spermatogenesis has been subdivided into seven stages, on the basis of both analysis of the morphological changes that the gonad undergoes during its development and the phases of germ cell differentiation (Fig. 8, Table 1).

Stages 1 and 2 are the first developmental stages corresponding to a proliferative or spermatogonial phase with growing gonad primordium through numerous cycles of mitotic divisions inside a syncytium and the generation of a definitive number of primary spermatocytes at stage 3. This event involves an enlargement of the testis, which reaches nearly the size of the mature testis, whereas somatic growth is arrested. The following stages, represented by stages 4 and 5 activity of meiosis and spermiogenesis, are brief and without volumetric variations in the testis. Stage 4 corresponds to the meiotic phase. The passage from spermatocytes to haploid spermatids was first described in detail in the present study and involves i) a progressive segregation of the latter from the syncytial mass with the formation of large intercellular bridges through which organelles migrate, and ii) a reduction of spermatid volume due to the compacting of the nuclear material and the remodelling of the cytoplasmic material. Stage 5 is a post-meiotic phase of early spermiogenesis that completes during stages 6 and 7 and rapidly forms functional spermatozoon by reshaping the cell, condensing chromatin, forming acrosome, and assembling flagellum. As a novelty with previous reports (Martinucci et al., 2005), the appearance of flagellum is late in comparison with that in ascidians, where the flagellum is still recognisable beginning from the spermatocyte stage (Cavey, 1994; Burighel and Martinucci, 2000). Cell debris discharge by the spermatids has never been observed, suggesting that almost all the material of the early spermatid is utilised for the assembly of both the

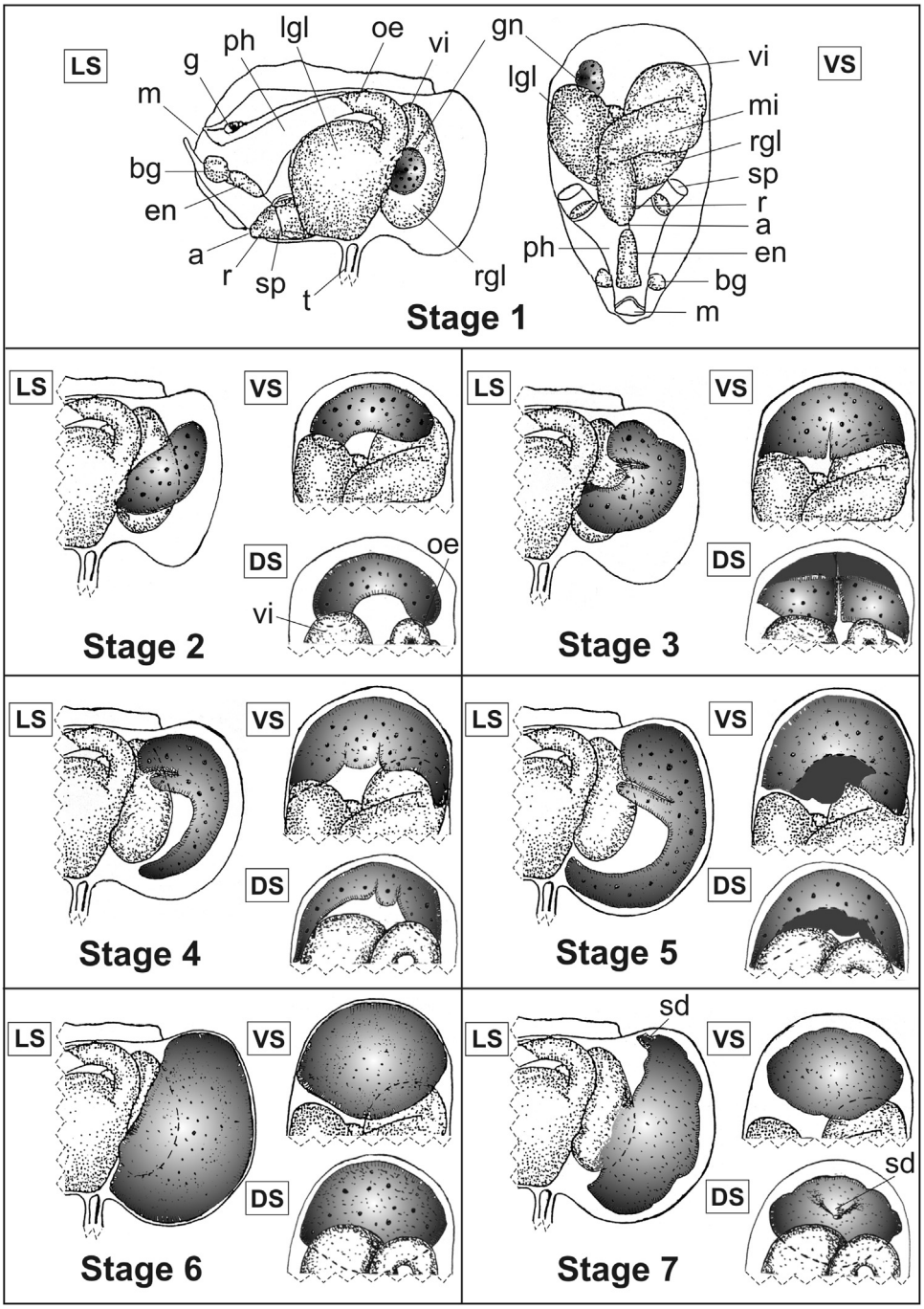

Fig. 8. Sketch of trunk of *Oikopleura dioica* showing internal anatomy from the left side (LS), ventral side (VS) and dorsal side (DS) at the various developmental stages of the male gonad. The wavy hatched line indicates anatomical parts not shown, i.e. the anterior part of the trunk and the distal part of the tail following its ventral attachment. a: anus; bg: buccal gland; en: endostyle; g: ganglion; gn: gonad; lgl: left gastric lobe; m: mouth; mi: mid-intestine; oe: oesophagus; ph: pharynx; r: rectum; rgl: right gastric lobe; sd: spermiduct; sp: spiracle; t: tail; vi: vertical intestine.

flagellum and the acrosome and for the volume increase of the mitochondrion, which first flanks the nucleus and in the latter stages moves posteriorly to it. Moreover, large nurse nuclei inside the syncytial structure together with the small ones of the germ cells have not been observed unlike reported for *Oikopleura cophocerca* (Bolles Lee, 1884) and the fritillarids *Fritillaria pellucida* and *Fritillaria borealis* (Martinucci et al., 2005). This suggests that, in *O. dioica*, the syncytial structure does not depend on the presence of trophic cells, which progressively degenerate, also in contrast with other invertebrates, such as Oligochaeta (Jamieson, 1981), and that the cytoplasmic material and organelles of the syncytial structure become part of the spermatids. It is well known that the cytoplasmic bridges in the ascidians play a key role in synchronising the clusters of isogenic cells and in exchanging materials and whole organelles between the connected cells. In the syncytium of the appendicularians, the bridges not only synchronise all germ cells but also allow the organelles, in particular, mitochondria, to migrate from the common cytoplasm towards the germ cells. The organelle migration is an intriguing phenomenon probably driven by cytoskeletal components like microfilament dynamics and microtubule motor proteins together with local change in cytoplasm fluidity.

Spermiogenesis is rapid and leads to the formation of a very differentiated spermatozoon, in which the nucleus is very small and sub-spherical in shape due to the late compacting of the chromatin and

Table 1
Principal diagnostic features of the seven stages of *O. dioica* testis development and spermatogenesis.

Stage	Spermatogenetic phase	Trunk length (mm)	Gross morphology of the testis	Histology of the testis	Type of germ cells
1	Proliferative	0.371 ± 0.032	70 μm high × 50 μm long; subspherical primordium (ovary or testis) contacting vertical intestine behind left gastric lobe.	Large undifferentiated germ cells with scarcely visible cellular boundaries and one couple of centrioles per cell.	Gonocytes
2	Proliferative	0.410 ± 0.037	100 μm high × 50 μm long; primordium growing dorsally and bent ventrally between gastric lobes.	Syncytium formed of sinuous, interconnected lobes, delimited by narrow spaces; presence of one type of spherical nuclei (2.2 μm in diameter) with nucleolus; two couples of centrioles per cell.	Spermatogonia
3	Pre-meiotic	0.468 ± 0.075	240 μm high × 120 μm long; presence of antero-dorsal protrusion increasing contact with right gastric lobe; dorsal large depression forming two symmetrical parts.	Syncytium forming lobes confined in spaces; germ cells moderately lengthened, connected peripherally by wide cytoplasmic bridges; large nuclei with chromatin condensed in peripheral clusters; absence of nucleolus.	Primary spermatocytes
4	Meiotic	0.546 ± 0.24	350 μm high × 180 μm long; asymmetric form for right part surrounding laterally and ventrally the right gastric lobe; secondary digitiform median protrusion between gastric lobes; presence of central cavity.	Syncytium forming a thin, anastomised network; germ cells as clusters of grapes; synaptonemal complexes in homogeneous nuclei; two couples of centrioles per cell.	Secondary spermatocytes
5	Spermiogenesis	0.843 ± 0.36	700 μm high × 340 μm long; maximal extension of both median protrusion and ventral wrapping of gastric lobes; reduction of central cavity.	Reduction of syncytial cytoplasm; very large confluent mitochondria crossing cytoplasmic bridges; subspherical nuclei (1 μm in diameter); acrosome and flagellum formation; one couple of centrioles per cell.	Early and intermediate spermatids
6	Spermiogenesis	0.942 ± 0.87	700 μm high × 550 μm long; maximal extension in the whole genital cavity.	Short syncytial structures with scanty mitochondria; tadpole-shaped germ cells; ring-shaped nuclei with plaque-condensed chromatin; presence of anterior and posterior nuclear channels; mid-piece appearance; distal centriole only.	Late spermatids
7	Spermiogenesis	0.984 ± 0.66	Before sperm ejection, size as stage 6; dorsal spermiduct appearance.	Disappearance of syncytial cytoplasm; three regions clearly distinguishable in mature sperm; head formed of a small nucleus with highly dense chromatin, a well-developed acrosome inside an anterior nuclear channel, and basal body of flagellum inside a posterior nuclear channel; mid-piece formed of a single mitochondrion located behind the nucleus and embracing the axoneme; tail represented by a long free portion of flagellum.	Spermatozoa

undergoes slight lengthening and a deep morphological change to form the posterior and anterior channels in which the flagellum and the acrosome, respectively, are inserted. The small size of the head of the spermatozoon containing little quantity of nuclear substance (oligopyrenic sperm) may be related to the high number of spermatozoa produced in a short time in the narrow space of the testis compacted inside the genital cavity (Holland et al., 1988). The paraxonemal localisation of mitochondrion in the mid-piece might be a consequence of the nuclear size reduction and is unique to tunicates. It comes from portions of the giant mitochondria inside the syncytium and, at the final maturity phase, first shifts laterally (intermediate spermatids, stage 5) and then posteriorly to the nucleus (late spermatids, stage 6) to form an open ring surrounding the flagellum, while, in the other tunicates, the mitochondria are small and numerous already inside the spermatogonia and then they are melted to form a larger one flanking the nucleus at the spermatid stage (Burighel and Martinucci, 2000). The formation of the acrosome is also particular. Among the other tunicates, only doliolids have an evident acrosome (Holland, 1989), whereas that of ascidians is very small (Jamieson, 1991). In the ascidians, the acrosome begins to form at the stage of early spermatids, with little variations among the various species (Fukumoto, 1986) but always with the formation of very small vesicles that melt at the apex of the spermatozoon. In the present study, the acrosome of *O. dioica* has been reported beginning from intermediate spermatids (stage 5), due to the activity of both the rough endoplasmic reticulum and the Golgi complex. It is assembled at the apex of the head and then moves into the anterior channel of the nucleus in the late spermatids (stage 6). Holland et al. (1988) reported that the acrosome of *O. dioica*, conspicuous in size, during egg fertilisation behaved similarly to that of the echinoderms because it formed an acrosomal process. At the level of the socket of the acrosome behind the nuclear membranes, a light space containing fibrillar material is detectable. It corresponds to the zone from which the acrosomal process emerges (Holland et al., 1988). This material, observed in TEM images, is probably G-actin, which, at the moment of egg fertilisation, polymerises in F-actin following a mechanism similar to that described for sea urchin (Vacquier, 1979). It is noteworthy that the appendicularian spermatozoa have a particular complex acrosome with respect to the scanty follicular cells covering the spawned eggs. This is remarkably different from other tunicates with external fertilisation, the eggs of which are covered by a multilayer specialised envelope (Jeffery, 1980), suggesting that, as occurs in echinoderms (Nakachi et al., 2006), the function of the acrosome may be not only the production of hydrolytic enzymes for overcoming the egg barrier but also the exposure of its internal membrane, which can contain the species-restricted recognition and interaction components for the gamete fusion in the pelagic environment (Miller and King, 1983).

According to Holland (1990, 1991), analysis of the morphological data of the mature germ cells of tunicates allows a ranking of the spermatozoa – from the less to the most specialised ones – in the order appendicularians < doliolids < solitary ascidians < compound ascidians < pyrosomes < salps. The appendicularians share with ascidians and thaliaceans the presence of only one mitochondrion and the lack of a proximal centriole, both considered plesiomorphic characters of tunicates. The synchronous spermatogenesis and the nucleus being penetrated by the basal body and the axoneme of the flagellum are instead apomorphic characters observed only in appendicularians. Despite the presence of primitive characters such as the large acrosome and the globular and compact nucleus, the appendicularian spermatozoon does not share at all the typical structures of the primitive sperm cell: the mitochondrion in the cylindrical mid-piece can be a derivative feature and not a plesiomorphic condition because the subsequent migration of the mitochondrion behind the nucleus. The morphology of the sperm suggests that the tunicates represent a monophyletic group and that the evolutionary pathway of appendicularians branched basally. The precocious divergence of appendicularians from the other tunicates is also supported by molecular phylogenetic analyses (Wada and Satoh, 1994; Wada, 1998; Holland, 2016; Kocot et al., 2018).

5. Conclusions

The proposed subdivision of spermatogenesis in seven stages appears valid to determine the differentiation of the testis *in toto* and sections because the only references to the gonad size itself or the time after metamorphosis are not a useful criterion for this purpose. Together with the timing of the differential expression of genetic markers, it could represent a tool for staging male individuals with greater certainty in both reared and pelagic populations.

Future efforts from comparative genomics and whole-genome transcription data analysis will be necessary for the establishment of a useful testis-differentiation staging with gene expression activation markers. To date, two well-defined examples are available for spermatogonial and spermiogenesis phases. During the proliferative or premeiotic phase (stages 1 and 2), *O. dioica* Cyclin D variants exhibit distinct temporal-spatial localisations during germ-line nuclear proliferation, as Cyclin Db and Dd variants are expressed in the nucleus and cytoplasm, respectively (Subramaniam et al., 2015). Expression of genes during spermiogenesis (stages 5–7) has been reported in OikoBase (Danks et al., 2013). In particular, GSOIDG00004881001 codes for a testis-specific serine/threonine-protein kinase 1 (TSSK-1). This protein kinase is expressed post-meiotically in mammals, where it has a role in sperm differentiation and functions during maturation, capacitation and fertilisation through phosphorylation events in signalling processes, which cause post-translational modifications of proteins (Hao et al., 2004). Other molecular markers proposed to participate in gonad development controlling spermatogenesis of *O. dioica* are i) sex-specific microRNAs (miRNAs), which appear as male/female gonad differentiation occurs (Fu et al., 2008), i.e., during transition from stage 1 to stage 2 of the present proposed classification, and ii) genome-wide shift in the mode of selection of male-specific transcription start sites together with enrichments of histone modifications (Danks et al., 2018).

Acknowledgements

The author wishes to thank the staff of the Station Zoologique, CEROV, Villefranche-sur-Mer (France) for facilities in supplying specimens. The author would also like to express deep gratitude to Prof. P. Burighel and G.B. Martinucci, her research mentors, who provided her with very valuable support, skilful suggestions and useful critiques for the improvement of this work. This research did not receive any specific grant from funding agencies in the public, commercial, or not-for-profit sectors. The English text was revised by American Journal Experts (AJE, http://www.journalexperts.com/, certificate #C9BF-CD44-BDBA-80F1–3F5F).

Declarations of interest

None.

References

Bolles Lee, A., 1884. Recherches sur l'ovogénèse et la spermatogénèse chez les Appendiculaires. Recu. Zool. Suisse 1, 645–663.

Bretsky, P.W., Lorenz, D.M., 1970. Adaptive response to environmental stability: A unifying concept in paleoecology. North Am. Paleont. Convention, Chicago, 1969, Proceedings E, 522–550.

Burighel, P., Cloney, R.A., 1997. Urochordata: Ascidiacea. In: Harrison, F.W., Ruppert, E.E. (Eds.), Microscopic Anathomy of Invertebrates, vol. 15, Hemichordata, Chaetognatha and the Invertebrate Chordates. John Wiley & Sons, Ltd., Chichester, 221–347.

Burighel, P., Martinucci, G.B., 2000. Urochordata. In: Jamieson, B.G.M. (Ed.), Reproductive Biology of Invertebrates, vol. 9, Part C, Progress in Male Gamete Ultrastructure and Phylogeny. John Wiley & Sons, Ltd., Chichester, 261–298.

Cañestro, C., Yokoi, H., Postlethwait, J.H., 2007. Evolutionary developmental biology and genomics. Nat. Rev. Genet. 8, 932–942.
Cavey, M.J., 1994. Spematogenesis in the ovotestis of the solitary ascidian *Boltenia villosa*. In: Wilson, W.H., Stricker, S.A., Shinn, G.L. (Eds.), Reproduction and Development of Marine Invertebrates. Johns Hopkins University Press, Baltimore, 64–76.
Colombera, D., Fenaux, R., 1973. Chromosome form and number in the Larvacea. Boll. Zool. 22, 183–185.
Danks, G.B., Campsteijn, C., Parida, M., Butcher, S., Doddapaneni, H., Fu, B., Petrin, R., Metpally, R., Lenhard, B., Wincker, P., Chourrout, D., Thompson, E.M., Manak, J.R., 2013. OikoBase: a genomics and developmental transcriptomics resource for the urochordate *Oikopleura dioica*. Nucleic Acids Res. 41, D845–D853, (Database issue).
Danks, G.B., Navratilova, P., Lenhard, B., Thompson, E.M., 2018. Distinct core promoter codes drive transcription initiation at key developmental transitions in a marine chordate. BMC Genom. 19, 164.
Denoeud, F., Henriet, S., Mungpakdee, S., Aury, J.-M., Da Silva, C., Brinkmann, H., Mikhaleva, J., Olsen, L.C., Jubin, C., Cañestro, C., Bouquet, J.-M., Danks, G., Poulain, J., Campsteijn, C., Adamski, M., Cross, I., Yadetie, F., Muffato, M., Louis, A., Butcher, S., Tsagkogeorga, G., Konrad, A., Singh, S., Jensen, M.F., Cong, E.H., Eikeseth-Otteraa, H., Noel, B., Anthouard, V., Porcel, B.M., Kachouri-Lafond, R., Nishino, A., Ugolini, M., Chourrout, P., Nishida, H., Aasland, R., Huzurbazar, S., Westhof, E., Delsuc, F., Lehrach, H., Reinhardt, R., Weissenbach, J., Roy, S.W., Artiguenave, F., Postlethwait, J.H., Manak, J.R., Thompson, E.M., Jaillon, O., Du Pasquier, L., Boudinot, P., Liberles, D.A., Volff, J.-N., Philippe, H., Lenhard, B., Crollius, H.R., Wincker, P., Chourrout, D., 2010. Plasticity of animal genome architecture unmasked by rapid evolution of a pelagic tunicate. Science 330, 1381–1385.
Fenaux, R., 1963. Ecologie et biologie des Appendiculaires méditerranéens. Vie Milieu 51, 106–112.
Fenaux, R., 1967. Les Appendiculaires. Faune de l'Europe et du Bassin Méditerranéenne. Masson et C.ie, Paris, 1–116.
Fenaux, R., 1976. Cycle vital d'un Appendiculaire *Oikopleura dioica* Fol, 1872, Description et cronologie.. Ann. Inst. Océan. Paris 52, 89–101.
Fenaux, R., Gorsky, G., 1983. Cycle vital et croissance de l'appendiculaire *Oikopleura longicauda* (Vogt), 1854. Ann. Inst. Oceanogr. Paris 59, 107–116.
Flood, P.R., Afzelius, B.A., 1978. The spermatozoon of *Oikopleura dioica* Fol, 1872 (Larvacea, Tunicata). Cell Tissue Res. 191, 27–37.
Franzén, A., 1970. Phylogenetic aspects of the morphology of spermatozoa and spermiogenesis. In: Baccetti, B., B (Eds.), Comparative Spermatology. Academic Press, New York, 29–45.
Franzén, A., 1983. Urochordata. In: Adiyodi, K.G., Adiyodi, R.G. (Eds.), Reproductive Biology of Invertebrates, vol. 2, Spermatogenesis and Sperm Function. John Wiley & Sons, Ltd., Chichester, 621–632.
Fu, X., Adamski, M., Thompson, E.M., 2008. Altered miRNA repertoire in the simplified chordate, *Oikopleura dioica*. Mol. Biol. Evol. 25, 1067–1080.
Fukumoto, M., 1986. The acrosome in ascidian. I: Pleurogona. Int. J. Invert. Rep. 10, 335–346.
Galt, C.P., 1972. Development of *Oikopleura dioica* (Urochordata: larvacea): Ontogeny of Behaviour and of Organ Systems Related to Construction and Use of the House (Ph.D. dissertation). Washington University, Seattle.
Galt, C.P., Fenaux, R., 1990. Urochordata: larvacea. In: Adiyodi, K.G., Adiyodi, R.G. (Eds.), Reproductive Biology of Invertebrates, vol. 4, Fertilization, Development, and Parental Care. John Wiley & Sons, Ltd., Chichester, 471–500.
Ganot, P., Bouquet, J.-M., Thompson, E.M., 2006. Comparative organization of follicle, accessory cells and spawning anlagen in dynamic semelparous clutch manipulators, the urochordate Oikopleuridae. Biol. Cell 98, 389–401.
Godeaux, J., Bone, Q., Braconnot, J.C., 1998. Anatomy of Thaliacea. In: Bone, Q. (Ed.), The Biology of the Pelagic Tunicates. Oxford University Press, Oxford, 1–24.
Grier, H., 1992. Chordate testis: the extracellular matrix hypothesis. J. Exp. Zool. 261, 151–160.
Hao, Z., Jha, K.N., Kim, Y.H., Vemuganti, S., Westbrook, V.A., Chertihin, O., Markgraf, K., Flickinger, C.J., Coppola, M., Herr, J.C., Visconti, P.E., 2004. Expression analysis of the human testis-specific serine/threonine kinase (TSSK) homologues. A TSSK member is present in the equatorial segment of human sperm. Mol. Hum. Reprod. 10, 433–444.
Holland, L.Z., 1988. Spermatogenesis in the salps *Thalia democratica* and *Cyclosalpa affinis* (Tunicata: thaliacea): An electron microscopic study. J. Morphol. 198, 189–204.
Holland, L.Z., 1989. Fine structure of spermatids and sperm of *Dolioletta gegenbauri* and *Doliolum nationalis* (Tunicata: thaliacea): Implications for Tunicata phylogeny. Mar. Biol. 101, 83–95.
Holland, L.Z., 1990. Spermatogenesis in *Pyrosoma atlanticum* (Tunicata: thaliacea): Implications for Tunicata phylogeny. Mar. Biol. 105, 451–470.
Holland, L.Z., 1991. The phylogenetic significance of tunicate sperm morphology. In: Bacetti, B. (Ed.), Comparative Spermatology 20 Years After. Sarono Symp. Publ. 75. Raven Press, New York, 961–965.
Holland, L.Z., 2016. Tunicates. Curr. Biol. 26, R146–R152.
Holland, L.Z., Gorsky, G., Fenaux, R., 1988. Fertilization in *Oikopleura dioica* (Tunicata, Appendicularia): acrosome reaction, cortical reaction and sperm-egg fusion. Zoomorphology 108, 229–243.
Jamieson, B.G.M., 1981. Reproductive systems, origin of gametes, spermatogenesis. In: The Ultrastructure of the Oligochaeta. Academic Press, London, 313–355.
Jamieson, B.G.M., 1991. Fish Evolution and Systematics: Evidence from Spermatozoa. Cambridge University Press, Cambridge, 1–48.
Jeffery, W.R., 1980. The follicular envelope of ascidian eggs: a site of messenger RNA and protein synthesis during early embryogenesis. J. Exp. Zool. 212, 279–289.
Kocot, K.M., Tassia, M.G., Halanych, K.M., Swalla, B.J., 2018. Phylogenomics offers resolution of major tunicate relationships. Mol. Phylogenet. Evol. 121, 166–173.
Martini, E., 1909. Über Eutelie und Neotenie. Verh. Dtsch. Zool. Ges. 1909, 292–299.
Martinucci, G., Brena, C., Cima, F., Burighel, P., 2005. Synchronous spermatogenesis in appendicularians. In: Gorsky, G., Youngbluth, M.J., Deibel, D. (Eds.), Response of Marine Ecosystems to Global Change: Ecological Impact of Appendicularians. Contemporary Publishing International, Paris, 113–123.
Meinertzhagen, I.A., 2005. Eutely, cell lineage, and fate within the ascidian larval nervous system: determinacy or to be determined? Can. J. Zool. 83, 184–195.
Miller, R., King, K.R., 1983. Sperm chemotaxis in *Oikopleura dioica* Fol, 1872 (Urochordata: larvacea). Biol. Bull. 165, 419–428.
Nakachi, M., Moriyama, H., Hoshi, M., Matsumoto, M., 2006. Acrosome reaction is subfamily specific in sea star fertilization. Dev. Biol. 298, 597–604.
Nikitin, V., 1929. La distribution verticale du plancton dans la Mer Noire. II. Zooplancton (Les Copépodes et les Cladocéres exceptés). Trav. Stat. Biol. Sebastopol Leningr. 1, 27–152.
Nishida, H., 2008. Development of the appendicularian *Oikopleura dioica*: culture, genome, and cell lineages. Dev. Growth Differ. 50, 239–256.
Nishino, A., Morisawa, M., 1998. Rapid oocyte growth and artificial fertilization of the Larvaceans *Oikopleura dioica* and *Oikopleura longicauda*. Zool. Sci. 15, 723–727.
Onuma, T.A., Isobe, M., Nishida, H., 2017. Internal and external morphology of adults of the appendicularian, *Oikopleura dioica*: an SEM study. Cell Tissue Res. 367, 213–227.
Paffenhöfer, G.A., 1973. The cultivation of an appendicularian through numerous generations. Mar. Biol. 22, 183–185.
Salensky, W., 1904. Etudes anatomiques sur les appendiculaires. I. *Oikopleura vanhoeffeni* Lohmann. II. *Oikopleura rufescens* Fol. III. *Fritillaria pellucida* Bisch. IV. *Fritillaria borealis* Lohmann. 13. Mém. Acad. Imp. Sci., St. Pétersbourg, 1–44.
Satoh, N., 2016. Comparative genomics of deuerostomes. In: Chordate Origins and Evolution: the Molecular Evolutionary Road to Vertebrates. Academic Press-Elsevier, London, 59–79.
Savelieva, A.V., Dautov, S. Sh, 2012. Formation and ultrastructural organization of gonads in *Oikopleura gracilis* Lohmann, 1896 (Urochordata: appendicularia). Russ. J. Mar. Biol. 38, 253–260.
Shiga, N., 1976. Maturity stages and relative growth of *Oikopleura labradoriensis* Lohmann (Tunicata, Appendicularia). Bull. Plankton Soc. Jpn. 23, 81–95.
Subramaniam, G., Campsteijn, C., Thompson, E.M., 2015. Co-expressed cyclin D variants cooperate to regulate proliferation of germline nuclei in a syncytium. Cell Cycle 14, 2129–2141.
Thompson, E.M., Kallesøe, T., Spado, F., 2001. Diverse genes expressed in distinct regions of the trunk epithelium define a monolayer cellular template for construction of the oikopleurid home. Dev. Biol. 238, 260–273.
Vacquier, V.D., 1979. The interaction of sea urchin gametes during fertilization. Am. Zool. 19, 839–849.
Wada, S., 1998. Evolutionary history of free-swimming and sessile lifestyles in urochordates as deduced from 18S rDNA molecular philogeny. Mol. Biol. Evol. 15, 1189–1194.
Wada, S., Satoh, N., 1994. Details of evolutionary history from invertebrates to vertebrates as deduced from sequences of 18S rDNA. Proc. Natl. Acad. Sci. USA 91, 1801–1804.